Comparison of post-stack seismic amplitude inversion methods to relative acoustic impedance

C. A. M. Assis* (CEP/UNICAMP), G. B. D. Ignácio (CEP/UNICAMP) and H. B. Santos (CEP/UNICAMP & INCT-GP)

Copyright 2017, SBGf - Sociedade Brasileira de Geofísica.

This paper was prepared for presentation at the 15^{th} International Congress of the Brazilian Geophysical Society, held in Rio de Janeiro, Brazil, 31 July to 3 August, 2017.

Contents of this paper were reviewed by the Technical Committee of the 15^{th} International Congress of the Brazilian Geophysical Society and do not necessarily represent any position of the SBGf, its officers or members. Electronic reproduction or storage of any part of this paper for commercial purposes without the written consent of the Brazilian Geophysical Society is prohibited.

Abstract

We discuss and compare two methodologies to estimated the relative acoustic impedance (RAI). One is the coloured inversion, and the other is a linearized relation between the seismic trace and the impedance, that provides a linear system to be solved for the RAI. Additionally, we investigate the performance of one direct technique and two iterative methods applied to resolving the linear system problem to estimate the RAI seismic section. The numerical experiments demonstrate that the coloured inversion can produce good RAI estimation and that the linear system approach can provide similar results. Tests with real data indicate that the linear system approach can provide a slightly better impedance section than the coloured inversion if the numerical methods applied to solve the linear system problem are optimally parametrized at the well-log position.

Introduction

Attributes are commonly employed to assist in the seismic data interpretation. One useful attribute is the acoustic impedance (AI) obtained from the seismic amplitudes inversion. The AI seismic sections facilitate the stratigraphic analysis because it is a rock property (Latimer et al., 2000). In some cases, the relative acoustic impedance (RAI) is enough to help in the thin layer reservoir characterization (Brown et al., 2008). The coloured inversion methodology (Lancaster and Whitcombe, 2000) is a computationally cheap and quite robust approach to estimate the RAI from the seismic data. This technique makes use of an operator derived at the well-log position to transform/invert the data to RAI. Hampson et al. (2005), proposed a simultaneous post-stack seismic amplitude inversion to absolute AI, in which a spike deconvolution and the seismic trace integration are performed in one step. Thus, given an initial low-frequency model, the absolute AI is estimated using a conjugate gradient algorithm to solve a linear relation between the seismic and the impedances logarithm. In this work, we adapt the Hampson et al. (2005) methodology to make it suitable for the RAI estimation. Different techniques to solve the linear system obtained are tested, and the results compared with the RAI produced by the coloured inversion. Tests on real seismic data indicate that the linear system approach can provide an impedance section with better event continuity than the coloured inverted data.

Theory

The coloured inversion methodology requires at least one well-log tied to the seismic data to build an operator in the frequency domain. The operator magnitude spectra is defined by the division between the average of the well-log RAI spectra and the average seismic spectra. Assuming the wavelet embedded in the seismic data is zero phase, the operator phase is set to -90°(Lancaster and Whitcombe, 2000). Finally, the derived operator is convolved with each seismic trace in the time-domain. Hampson et al. (2005) proposed a post-stack inversion to AI that makes use of the convolutional model and the assumption of small reflectivity for the zero incidence angle P-wave reflection coefficient. Then with an initial guess for the impedance model, the conjugate gradient together with the linear relation between the seismic and the impedance logarithm can be used to estimate the absolute impedance. Now, we look in more detail the Hampson et al. (2005) approach. The zero incidence angle P-wave reflection coefficient is given by

$$R_i = \frac{AI_{i+1} - AI_i}{AI_{i+1} + AI_i}, \tag{1}$$

where R_i is the reflection coefficient from the boundary between the rock layers with impedance AI_{i+1} and AI_i. Rearranging equation 1 and taking the natural logarithm

$$\ln AI_{i+1} = \ln AI_i + \ln(1+R_i) - \ln(1-R_i). \tag{2}$$

Knowing that $\ln(1+x) \approx x$ for $x \approx 0$, it follows that

$$R_i \approx \frac{1}{2}\left[\ln AI_{i+1} - \ln AI_i\right], \tag{3}$$

that is the small reflectivity equation. In practice, it works well for $|R| < 0.3$ (Oldenburg et al., 1983). Equation 3 was obtained by linearizing the reflection coefficient logarithm. We propose to include the expansion of the impedance logarithms in a Taylor series around one and retaining only the first order term. In order to approximately satisfy this Taylor series assumption, the impedance is normalized with a reference value AI_{ref} such as the impedance profile maximum absolute value. Considering that our objective is to estimate the RAI, the proposed normalization is not an issue since we are not concerned with the real impedance magnitude, but the primary information that we want to extract is the RAI increase or decrease in a neighborhood. Therefore, considering $RAI/RAI_{ref} \approx 1$ and knowing that $\ln(z) \approx z-1$ for $z \approx 1$, we obtain

$$\widetilde{R}_i \approx \frac{1}{2RAI_{ref}}\left[RAI_{i+1} - RAI_i\right], \tag{4}$$

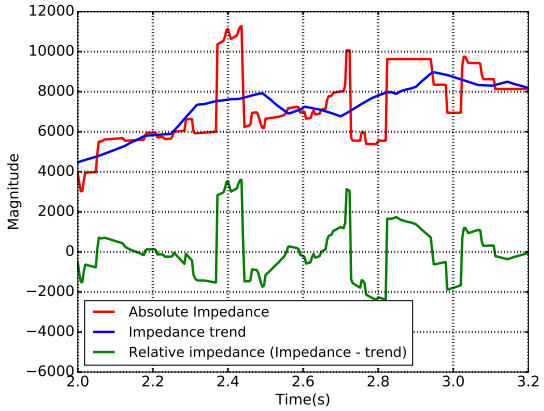

Figure 1: Example of absolute acoustic impedance and relative acoustic impedance. The RAI is obtained by subtracting the trend from the absolute AI. The measurements initially in depth were converted to two-way traveltime. Data extracted from the Marmousi2 model (Martin et al., 2006).

where $\widetilde{R}_i$ is the frequency band-limited reflection coefficient obtained from the RAI. Figure 1 illustrates the relationship between the absolute AI and the RAI. The absolute AI in each position is the exact rock property that would be obtained from the product between the compressional velocity and the density of a rock sample, which is always a positive quantity. On the other hand, the RAI mainly provides information about the increase or decrease of the impedance and it can be negative. Note that the RAI is obtained by subtracting the trend from the absolute AI. In the frequency domain, the RAI is the absolute AI without the low-frequency content. Moreover, if the RAI is estimated from the seismic data, the high-frequency content is also missing due to the seismic band-limitation. Having said that, we claim that although equation 4 may be a less precise approximation than equation 3 to the exact zero incidence reflection coefficient, it is more suitable to deal with the RAI because it does not make use of the logarithm function, this way, preventing problems with zeros and negative values. The equation 4 can be written in matrix form using the difference operator

$$D = \begin{bmatrix} -1 & 1 & 0 & \cdots \\ 0 & -1 & 1 & \cdots \\ \vdots & \vdots & \ddots & \\ . & . & . & . \end{bmatrix} \tag{5}$$

then

$$\begin{bmatrix} \widetilde{r_1} \\ \widetilde{r_2} \\ \vdots \\ \widetilde{r_N} \end{bmatrix} \approx \frac{1}{2} \begin{bmatrix} -1 & 1 & 0 & \cdots \\ 0 & -1 & 1 & \cdots \\ \vdots & \vdots & \ddots & \\ . & . & . & . \end{bmatrix} \begin{bmatrix} RAI_1/RAI_{ref} \\ RAI_2/RAI_{ref} \\ \vdots \\ RAI_N/RAI_{ref} \end{bmatrix} \tag{6}$$

The convolutional model is defined by

$$\mathbf{s} = \mathbf{w} * \mathbf{r} + \mathbf{n}, \tag{7}$$

where $\mathbf{s}$ is the seismic signal, $\mathbf{w}$ is the wavelet embedded in the seismic trace, $*$ denotes the convolution operation, $\mathbf{r}$ is the reflection coefficient sequence, and $\mathbf{n}$ is additive noise. Rewriting the convolutional model in matrix form, for instance discarding the noise component, and substituting equation 6

$$\mathbf{s} = \frac{1}{2} W D \mathbf{x}, \tag{8}$$

where W is a Toeplitz matrix build with the wavelet and the vector $\mathbf{x}$ is the normalized RAI profile. Equation 8 is a linear relationship between the seismic signal $\mathbf{s}$ and the impedances $\mathbf{x}$. Defining

$$A = \frac{1}{2} W D, \tag{9}$$

equation 1 can be rewritten as

$$A\mathbf{x} = \mathbf{s}. \tag{10}$$

In practice, while solving the linear system 10 it is being performed a spike deconvolution and a seismic trace integration simultaneously. As a consequence, the matrix A is ill-conditioned as any seismic deconvolution problem involving a frequency band-limited wavelet. When the matrix A is nonsingular, direct methods as *Gaussian Elimination* or QR decomposition may be used to solve the linear system 10. Furthermore, depending on the special properties of the matrix A, other efficient methods like Cholesky decomposition (when the matrix is positive definite) could be used. However, when the matrix A is singular, and this how we will handle our problem, the linear system 10 does not have a unique solution. When it happens, despite the case where the linear system doesn't have solutions (which is not the case of our particular problem), the linear system 10 has infinite solutions. If $\mathbf{x}$ is a solution of the linear system 10, then $\mathbf{x}$ is also a solution of the normal system

$$A^T A\mathbf{x} = A^T \mathbf{s}, \tag{11}$$

where A^T is the transpose of A. A vector $\mathbf{x}$ is the solution of the linear system 11 if, and only if, $\mathbf{x}$ is also the solution of the least square problem (Trefethen and Bau III, 1997)

$$\|\mathbf{s} - A\mathbf{x}\|_2 = \min_{w \in \mathbb{R}^n} \|\mathbf{s} - Aw\|_2. \tag{12}$$

If $\text{rank}(A) < n$, then the solution of the least square problem 12 is not unique (Watkins, 2004). In other words, there are many $\mathbf{x}$ for which $\|\mathbf{s} - A\mathbf{x}\|_2$ is minimized. The minimum-norm solution of the problem 12, consequently, the solution of the system 11 is given by $\mathbf{x} = A^\dagger \mathbf{s}$, where $A^\dagger$ denotes the pseudo-inverse of the matrix A (Golub and Kahan, 1965). Consider the SVD decomposition of the matrix $A \in \mathbb{R}^{n \times n}$, with $\text{rank}(A) = r \leq n$:

$$A = U \Sigma V^T, \tag{13}$$

where $U \in \mathbb{R}^{n \times n}$ and $V \in \mathbb{R}^{n \times n}$ are orthogonal matrices and $\sigma \in \mathbb{R}^{n \times n}$ is a diagonal matrix such that $diag(\Sigma) = \{\sigma_1, \sigma_2, \ldots, \sigma_r, 0, \ldots\}$, where σ_i, $i = 1, \ldots, r$, denotes the singular values of A, with $\sigma_1 \geq \sigma_2 \geq \ldots \geq \sigma_r \geq 0$. The pseudo-inverse of A might be written in terms of its SVD decomposition:

$$A^\dagger = V \Sigma^\dagger U^T, \tag{14}$$

where the diagonal matrix $\Sigma^\dagger \in \mathbb{R}^{n \times n}$ is the pseudo-inverse of Σ, with diagonal elements given by $diag(\Sigma^\dagger) = \{\sigma_1^{-1}, \sigma_2^{-1}, \ldots, \sigma_r^{-1}, 0, \ldots\}$ (Golub and Van Loan, 2012).

Theoretically, there is a remarkable difference between singular and nonsingular matrices. In other words, in the absence of roundoff errors during calculations, the singular value decomposition reveals the rank of the matrix. However, the presence of numerical errors turns the problem of determining the rank of a matrix harder, as might appears small singular values that theoretically would be zero (Watkins, 2004). Then, roughly speaking, it's necessary to consider a tolerance parameter ε that plays the following role: singular values σ_i lesser than ε are not considered, as they would be zero in the absence of numerical errors. So ordering the singular values of A such that $\sigma_1 \geq \sigma_2 \geq \ldots \geq \sigma_r \geq \varepsilon \geq \sigma_{r+1} \geq \ldots$, then the rank of A is assumed to be r. The application of the SVD decomposition to solve linear systems is considered a direct method and, in the absence of roundoff errors, provides the exact minimum-norm solution of the problem 12. Nevertheless, when large matrices are considered, the SVD approach might become computationally expensive. Furthermore, when the matrix is also sparse, the use of iterative methods becomes more efficient (Greenbaum, 1997). Although the application of iterative methods in our particular case does not provide the exact minimum-norm solution of the problem 12, they can generate an approximate solution of the system 10.

Methodology

Our objective is to compare different methods to estimate the RAI from the seismic data. One approach will be via the coloured inversion and the second will be via solving the linear system 10. In this paper, we consider the SVD that is a direct method and two different iterative methods, the traditional conjugate-gradient and the randomized Kaczmarz method. The pseudo-inverse of the matrix A, calculated with the SVD, will be obtained by discarding singular values smaller than a threshold. The threshold will be defined by testing a range of cutoff parameters and verifying which pseudo-inverse applied to the seismic trace nearest to the tied well-log data provides the highest correlation between the estimated RAI and the impedance from the well-log. A similar methodology will be applied to the iterative methods, but the parameter to be defined will the number of iterations. Additionally, the initial model will be the -90° rotated seismic trace, that can be understood as a simplified version of the coloured inverted data. For completeness, the iterative methods that will be used are discussed in more detail. The conjugate-gradient method has been already proposed by (Hampson et al., 2005) to solve the problem under investigation. Thus, it is going to be included in our tests. The conjugate-gradient method, which is a particular example of *Krilov* subspace method, is a variation on the steepest descent method (Greenbaum, 1997). However, the conjugate-gradient uses information from the last iteration, providing better performance. The conjugate-gradient works with positive definite matrices, expending less effort to generate the solution in comparison with the *Cholesky* decomposition (Watkins, 2004). Here, we use the conjugate gradient for least squares (CGLS) as discussed in Scales (1987). The Kaczmarz's method (Natterer, 2001), also known under the name Algebraic Reconstruction Technique (ART), commonly used in geophysical tomography, performs operations only in the rows of the system, which turns this method very useful if the matrix is sparse. Briefly, the classical scheme of Kaczmarz's method works through all the rows of A in a cyclic manner, projecting in each step the last iterate orthogonally onto the solution hyperplane generated by the i-th row of the system, that is: $a_i^T \mathbf{x} = s_i$, where a_i denotes the i-th row of A. It has been showed, however, that the rate of convergence of the Kaczmarz's method is improved when the algorithm works through the rows of A in a random manner, rather than sequentially (Natterer, 2001; Herman and Meyer, 1993). For this reason, in this paper, we are going to use the randomized Kaczmarz's method. Given an initial point $\mathbf{s_0}$, the randomized Kaczmarz's method performs the following calculations:

$$x_{k+1} = x_k + \left(\frac{s_{ri} - a_{r(i)}^T x_k}{a_{r(i)}^T a_{r(i)}}\right) a_{r(i)}, \tag{15}$$

where r(i) is chosen from the set {1, 2, . . . , n} at random, with probability proportional to the Euclidian norm of $a_{r(i)}$. The second part on the right of equation 15 is the orthogonal projection mentioned above.Note that the algorithm does not need to know the whole system, but only a small random part of it. Then, when the matrix is very sparse and well-posed, the computations in equation 15 are cheap, and the method may outperform most of the known iterative methods (Strohmer and Vershynin, 2009).

Application to Marmousi model

The Marmousi2 model (Martin et al., 2006) was used to assess each methodology to estimate the RAI. The exact absolute AI model and the correspondent reflection coefficient data, originally on depth domain, were transformed to the two-way travel time. The trend from the AI model was removed to obtain its RAI version. The calculations were made at the Marmousi2 trace position 751. The inversion techniques were evaluated using a seismic trace calculated by convolving the exact reflectivity series with a Ricker wavelet at 25-Hz peak frequency. Thus, the seismic data to be inverted contained only primary reflections and the biggest obstacle in the process to recover the exact RAI, in theory, should be only the seismic frequency band-limitation. The coloured inversion produced a RAI close to the exact model (Figure 2a). The magnitudes from the estimated RAI did not match the exact model, probably, due to the seismic data band-limitation. In general, the RAI estimated via the linear system solution performed, Figures 2b-2d, slightly better than the coloured inversion, Figure 2a. The correlation coefficients in Table 1 confirm that solving the linear system for the RAI was a little bit more precise than the coloured inversion. It is worth mentioning that the SVD result shown here was obtained by using a cutoff singular value of 0.004 and the testing range was from 10^{-5} to 1. The CGLS algorithm was parametrized with 150 iterations and the Kaczmarz with 10^6 line operations. The linear system solved had 500 lines, so in comparison with the CGLS technique, the Kaczmarz algorithm performed about 2000 iterations. The Kaczmarz also expended more time to solve the system than the CGLS algorithm, given the number of iterations necessary to achieve nearly the same correlation with the well-log for the seismic trace inverted to RAI near the well-log position. The SVD cutoff singular value and the iterative methods number of iterations were chosen as discussed in the Methodology section.

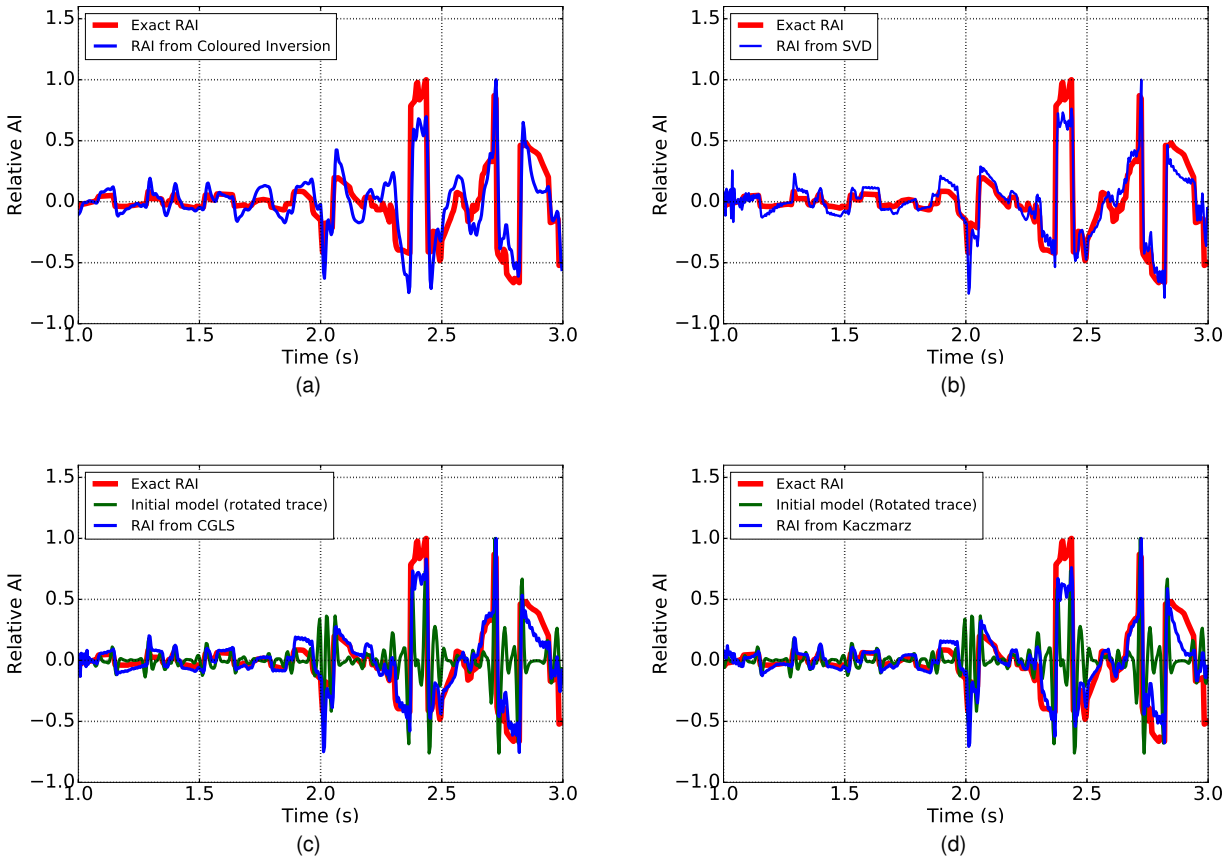

Figure 2: RAI from the Marmousi2 model at trace number 751. In red the exact RAI model and blue the estimated impedance. (a) Coloured inverted data. Results from linear system solution: (b) SVD; (c) CGLS with the initial solution in green; (d) Kaczmarz with the initial solution in green.

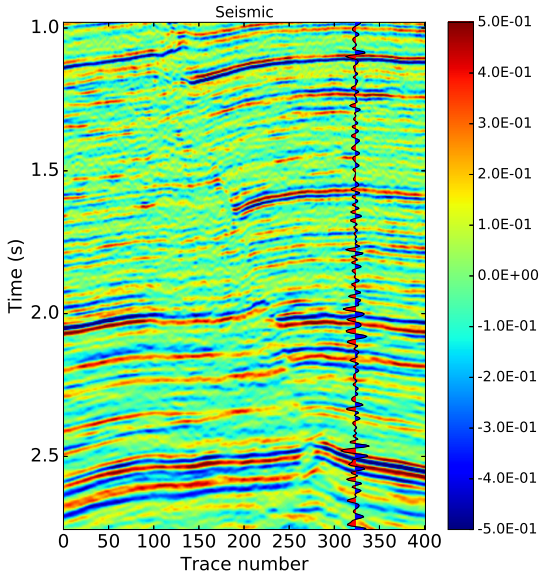

Figure 3: Seismic data and the synthetic seismic trace calculated by the convolution between the reflectivity estimated from the tied well-log and a 25-Hz Ricker wavelet.

Application to real data

We tested the inversion methodologies on a real data composed of a sonic and density log from the Penobscot L-30 well and a stacked seismic section offshore from Nova Scotia, Canada (Bianco, 2014). We considered only the time window around valid well-log values. The seismic data frequency bandwidth is similar to the 25 Hz Ricker wavelet. Figure 3 exhibits the seismic data and synthetic trace calculated from the tied well-log. Figure 4 shows the inversion results, where the red arrows indicate the positions where the well-log RAI is in agreement with the inverted seismic data. The coloured inversion provided an interesting RAI section, which it is in agreement with the well-log in various positions (Figure 4b). Comparing the seismic section, Figure 3, and the RAI section, Figure 4b, it is clear that the inversion filled the space between neighbor reflections all over the data. In other words, the information was transformed from a boundary measurement to an interval representation. The SVD technique applied to solve the linear system approach performed well. Although it was applied trace by trace, the estimated RAI section presented events with higher continuity, Figure 4b, than the coloured inversion (Figure 4a). The black arrows in Figure 4 indicate the positions where the events continuity was

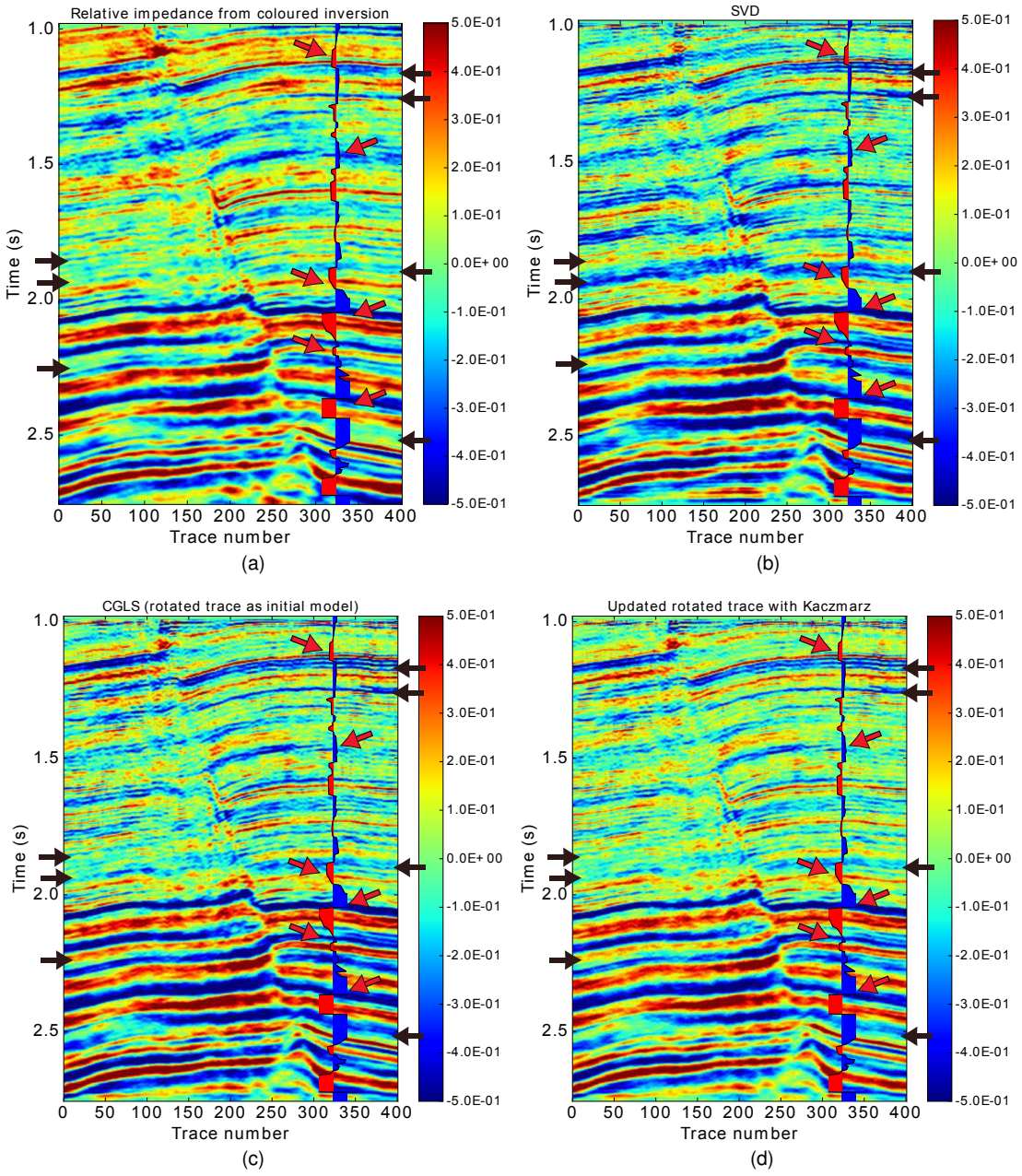

Figure 4: Real data and the tied well-log transformed to RAI. The red arrows indicate the positions where the well-log RAI is in agreement with the inverted seismic data. (a) Coloured inversion. Followed by the linear system problem solved with: (b) SVD; (c) Seismic -90° rotated + CGLS; (d) Seismic -90° rotated + Kaczmarz.

improved compared to the coloured inversion (Figure 4a). A drawback of the SVD approach was that it favored the negative RAI values over the positive ones in the data region from 1.0 to 1.8 seconds, (Figure 4b), while the coloured inversion produced an impedance section more balanced between the positive and negatives values. The CGLS and Kaczmarz techniques provided nearly the same RAI sections (Figures 4a and 4b). These results showed better layer continuity in some positions compared to the coloured inversion. But, the positive RAI values were slightly reduced, concerning the coloured inverted data, in the time window from 1.0 to 1.8 seconds. This observation is similar to the one made with the SVD results, but the CGLS and Kaczmarz techniques did not enhance the negative RAI values as the SVD method. Moreover, the CGLS and Kaczmarz lateral continuity improvement are nearly the same as the one produce by the SVD solution. It is worth noting that the CGLS result was obtained with 20 iterations and the Kaczmarz number of row operations divided by the solved system number of lines was about 65 iterations. Furthermore, the Kaczmarz expended more time than the CGLS to solve the linear system to achieve approximately the same correlation coefficient with the well-log data. Table 1 exhibits the correlation coefficient between the estimated RAI near the well-log correlated and the well-log measurement. For the techniques used to

Table 1: Correlation of the inverted seismic data to RAI with the exact relative impedance for each inversion approach. The left column displays the results from the Marmousi2 model and the right column the results from the tests with real data at the well-log position.

Method	Correlation	
	Marmousi	Real data
Coloured inversion	0.80	0.16
SVD	0.87	0.20
CGLS	0.89	0.15
Kaczmarz	0.86	0.15

solve the linear system, these are the optimal correlation coefficients. The SVD solution to the linear system approach obtained the highest correlation and the other approaches achieved approximately the same correlation coefficient. This result is in agreement with the visual inspection of the results exhibited in Figure 4, where the SVD result seems to be a little bit better than the others.

Discussion

The coloured inversion produced a good RAI section in the tests with numerical and real data. The numerical tests with the linear system approach produced results closer to the exact response than the coloured inversion, independently of the numerical method chosen to solve the problem. But analyzing closer the iterative methods, the Kaczmarz expended more time to solve the linear system than the CGLS algorithm. In the tests with real data, the SVD technique parametrized with an optimal cutoff singular value determined at the well-log position produced a RAI with higher correlation coefficient to the well-log measurement than the coloured inversion and the iterative methods. In the real data set used here, the SVD favored the negative RAI values in some parts of the inverted seismic data while the coloured inversion produced a RAI section with more balanced positive and negative RAI values. Again, the Kaczmarz was took more time than the CGLS technique to solve the linear system.

Conclusions

We compared two methodologies to estimate the relative acoustic impedance. One approach was the coloured inversion that uses well-log information to derive an operator to transform the seismic data to the RAI. The second was by using a linear relation between the seismic data and the RAI. Then we investigated one direct method and two iterative methods to solve the linear system obtained. The methodology discussed, demonstrated that well-log information can be used to calibrate the SVD and iterative methods like the CGLS and the Kaczmarz to produce results similar to the coloured inversion. But we highlight, that between the iterative schemes, the CGLS technique expended less time than the Kaczmarz to achieve the same accuracy level of the inverted seismic data at the well-log position. The convergence and efficiency of both methods applied to the problem stated here need to be further investigated. The SVD method used to solve the linear system approach can produce a slightly better RAI section from post-stack seismic data than the coloured inversion. Even tough, we suggest that both approaches should be taken into account in an interpretation project that makes use of the RAI. Additionally, we argue that as the inversion is applied trace by trace and considering the usual seismic traces number of samples, the SVD algorithm performance may not be a problem in the inversion of an entire seismic volume.

Acknowledgments

The authors are grateful to Petrobras, ANP, PFRH-PB15, PFRH-PB230 and FAPESP for the financial support and the scholarships. Additional support was provided by the sponsors of the *Wave Inversion Technology (WIT) Consortium*. The authors are also grateful to Lúcio Tunes Santos and Edwin Fagua Duarte for the valuable discussions.

References

Bianco, E., 2014, Geophysical tutorial: Well-tie calculus: The Leading Edge, **33**, 674–677.

Brown, L. T., J. Schlaf, and J. Scorer, 2008, Thin-bed reservoir characterization using relative impedance data, joanne field, u.k.: Presented at the 70th EAGE Conference and Exhibition incorporating SPE EUROPEC 2008, EAGE Publications.

Golub, G., and W. Kahan, 1965, Calculating the singular values and pseudo-inverse of a matrix: Journal of the Society for Industrial and Applied Mathematics, Series B: Numerical Analysis, **2**, 205–224.

Golub, G. H., and C. F. Van Loan, 2012, Matrix computations: **3**.

Greenbaum, A., 1997, Iterative methods for solving linear systems.

Hampson, D. P., B. H. Russell, and B. Bankhead, 2005, Simultaneous inversion of pre-stack seismic data: Presented at the SEG Technical Program Expanded Abstracts 2005, Society of Exploration Geophysicists.

Herman, G. T., and L. B. Meyer, 1993, Algebraic reconstruction techniques can be made computationally efficient (positron emission tomography application): IEEE transactions on medical imaging, **12**, 600–609.

Lancaster, S., and D. Whitcombe, 2000, Fast-track 'coloured' inversion: Presented at the SEG Technical Program Expanded Abstracts 2000, Society of Exploration Geophysicists.

Latimer, R. B., R. Davidson, and P. van Riel, 2000, An interpreter's guide to understanding and working with seismic-derived acoustic impedance data: The Leading Edge, **19**, 242–256.

Martin, G. S., R. Wiley, and K. J. Marfurt, 2006, Marmousi2: An elastic upgrade for marmousi: The Leading Edge, **25**, 156–166.

Natterer, F., 2001, The mathematics of computerized tomography.

Oldenburg, D. W., T. Scheuer, and S. Levy, 1983, Recovery of the acoustic impedance from reflection seismograms: Geophysics, **48**, 1318–1337.

Scales, J. A., 1987, Tomographic inversion via the conjugate gradient method: Geophysics, **52**, 179–185.

Strohmer, T., and R. Vershynin, 2009, A randomized kaczmarz algorithm with exponential convergence: Journal of Fourier Analysis and Applications, **15**, 262.

Trefethen, L. N., and D. Bau III, 1997, Numerical linear algebra: **50**.

Watkins, D. S., 2004, Fundamentals of matrix computations: **64**, 640.